Applied Catalysis B: Environmental 160–161 (2014) 247–253

Contents lists available at ScienceDirect

Applied Catalysis B: Environmental

journal homepage: www.elsevier.com/locate/apcatb

Enhanced photocatalytic oxidation of arsenite to arsenate in water solutions by a new catalyst based on MoO_x supported on TiO_2

V. Vaiano[a], G. Iervolino[a], D. Sannino[a,*], L. Rizzo[b], G. Sarno[a], A. Farina[b]

[a] Department of Industrial Engineering, University of Salerno, via Giovanni Paolo II, 132, 84084 Fisciano, SA, Italy
[b] Department of Civil Engineering, University of Salerno, via Giovanni Paolo II, 132, 84084 Fisciano, SA, Italy

ARTICLE INFO

Article history:
Received 25 March 2014
Received in revised form 12 May 2014
Accepted 18 May 2014
Available online 25 May 2014

Keywords:
Photocatalytic reaction
Arsenic
MoO_x/TiO_2
Mo loading
Reaction mechanism

ABSTRACT

Photocatalytic oxidation of As(III) to As(V) was investigated using a new catalyst based on molybdenum oxide supported on titania (MoO_x/TiO_2), under different irradiation intensities and catalyst dosages. Photocatalysts were prepared by incipient wet impregnation of anatase titania with ammonium heptamolybdate solutions. The obtained samples were characterized by thermogravimetric analysis, N_2 adsorption at −196 °C, X-ray diffraction, Laser Raman spectra and UV–vis reflectance spectra. UV–vis DRS spectra of the photocatalysts evidenced that the surface coverage with MoO_x did not significantly decrease the equivalent band gap energies. X-ray diffraction analysis showed that up to 8.4 wt% Mo-loading, molybdenum oxide remains on the surface of titania support as amorphous phases. Raman spectra showed the presence of hydrated octahedrally molybdate anchored species interacting with TiO_2 surface and a molybdenum oxide monolayer coverage of corresponding to about 9.8 wt% of MoO_3. Photocatalytic oxidation tests showed that TiO_2 alone is not able to oxidize all As(III) present in solution, while the complete conversion of As(III) to As(V) was achieved in the presence of MoO_x/TiO_2 catalyst. In particular, the best conversion was observed within 60 min of exposure to UV light irradiation with a Mo-loading corresponding to a monolayer coverage. As(V) produced during the photoreaction was completely released into solution, thus not occupying stably the active sites which results in a photocatalyst with high stability over the time.

1. Introduction

Arsenic contamination in groundwater and soil has become a serious health risk for humans. Among different arsenic oxidation states, arsenite (As(III)) is more toxic than arsenate (As(V)), and because of its high mobility and low affinity for adsorbents, tends to have long persistence during water treatment [1]. Possible approach in the removal of arsenic from water includes a pre-oxidation step of As(III) to As(V) and a subsequent removal of As(V) by a separation process (such as coagulation/precipitation, ion exchange, lime softening and adsorption). Unfortunately, typical chemicals used in the pre-oxidation step (e.g., ozone, chlorine, chlorine dioxide) result in the formation of dangerous oxidation/disinfection by products [2] and some separation methods (namely coagulation/precipitation and lime softening) have different drawbacks related to sludge treatment and disposal. Therefore, the development for efficient processes for the oxidation of As(III) into As(V) have been required to reduce toxicity and enhance subsequent removal by adsorbents. In this respect, photocatalytic oxidation with TiO_2, as a semiconductor, is effective in destroying a wide range of contaminants in gaseous and aqueous phases [3–15].

The photocatalytic conversion of As(III) to As(V) in the presence of TiO_2 alone has already been reported [16,17], however, TiO_2 adsorbs As(V) produced from the photoreaction leading to a progressive deactivation of the catalytic system [18,19]. Moreover, the low photonic efficiency has always been the major problem. The photocatalytic activity of TiO_2 can be greatly enhanced by doping catalysts with noble metals (as Pt) to facilitate the charge separation and interfacial electron transfer. However, the high cost of noble metals limits the practical applications [20]. An alternative way to enhance the photocatalytic reaction rate, is adding cheaper transition metals, such as V, Mo, Ru or Au on TiO_2 surface [14,21–25]. To our knowledge, no papers regarding the photocatalytic oxidation of As(III) on TiO_2 functionalized with transition metals has been published. In this work a purposely prepared new catalyst, namely MoO_x/TiO_2, was investigated in the photocatalytic oxidation of As(III) to As(V) in water. The catalyst was prepared by incipient wet impregnation of anatase titania with ammonium heptamolybdate

* Corresponding author. Tel.: +39 089 964092; fax: +39 089 9694057.
E-mail address: dsannino@unisa.it (D. Sannino).

http://dx.doi.org/10.1016/j.apcatb.2014.05.034
0926-3373/

Table 1
List of catalysts with their characteristics.

Catalyst	Nominal MoO_3 content (wt%)	Estimated MoO_3 content[a] (wt%)	SSA (m^2/g)	E_{bg}[b] (eV)	TiO_2 average crystallites size[c] (nm)
TiO_2	0	0	70	3.4	19
2Mo	2.4	2.02	70	3.4	18
6Mo	5.7	5.8	70	3.3	18
10Mo	9.8	8.4	65	3.3	18
15Mo	14.7	14.8	60	3.3	18

[a] Evaluated by TG–DTG analysis.
[b] Evaluated from UV–vis DRS analysis.
[c] Evaluated from XRD analysis.

solutions. The obtained samples were characterized by thermogravimetric analysis, N_2 adsorption at −196 °C, X-ray diffraction, Laser Raman spectra and UV–vis reflectance spectra. Photocatalytic activity was investigated under different irradiation intensities and catalyst dosages.

2. Materials and methods

2.1. Photocatalyst preparation and characterization

Anatase phase titania (PC105) was impregnated with ammonium heptamolybdate solutions. The resulting MoO_x/TiO_2 catalysts were then dried at 120 °C and calcined in air at 400 °C for 3 h. Specific surface areas (SSA) of the samples were evaluated by N_2 adsorption with a Costech Sorptometer 1042 after a pretreatment at 180 °C for 1 h in He flow (99.9990%). The Raman spectra of catalysts were recorded with a Dispersive MicroRaman system (Invia, Renishaw), equipped with 785 nm diode-laser, in the range 100–2500 cm^{-1} Raman shift. X-ray diffraction (XRD) measurements were realized using an X-ray micro diffractometer Rigaku D-max-RAPID, using Cu-Kα radiation. UV–vis reflectance spectra of powder catalysts were recorded by a Perkin Elmer spectrometer Lambda 35 using a RSA-PE-20 reflectance spectroscopy accessory (Labsphere Inc., North Sutton, NH). All spectra were obtained using an 8° sample positioning holder, giving total reflectance relative to a calibrated standard SRS-010-99 (Labsphere Inc., North Sutton, NH). The reflectance data were reported as the $F(R\infty)$ value from Kubelka–Munk theory vs the wavelength. Band gap determinations were based on a selection of the analytical methods present in the literature and applied in a properly selected range for a reproducible and comparable evaluation of absorption band edge. The evaluations were made by plotting $[F(R\infty) \times h\nu]^2$ vs $h\nu$ (eV) and calculating the x intercept of a line passing through $0.5 < F(R\infty) < 0.8$. Thermogravimetric analysis (TG–DTG) of samples was carried out in air flow with a thermo balance (SDT Q600, TA Instruments) in the range 20–1000 °C at 10 °C min^{-1} heating rate.

2.2. Photocatalytic activity tests

Photocatalytic activity tests were carried out with a reactor consisting of a pyrex cylindrical batch reactor (14.0 cm in diameter) filled in with 500 mL of solution. The aqueous solution was continuously stirred placing the reactor on a plate with a magnetic stirrer. The light source was a UV lamp (nominal power: 125 W, provided by Philips), and was placed at different distances from the surface of the solution, at 15, 10 and 5 cm (incident photon flux in the range 7.5–25.5 W/m^2). The catalyst dosage was in the range 0.1–0.5 g/L. The initial concentration of As(III) was 5 mg/L prepared by mixing 1.33 mL of Sodium Arsenite (0.05 mol/L) in 1 L distilled water. The suspension was left in dark condition for 1 h to evaluate the catalytic activity in the absence of irradiation. Photocatalytic reaction was carried under UV light up to 2 h. Slurry samples were collected at fixed time intervals, and filtered (pore size: 0.45 μm) for removing photocatalyst before analytical measurements.

2.3. Analytical measurements

The total arsenic concentration in the solution was analyzed by inductively coupled plasma spectrometry (ICP-OES, Thermo Fisher). The As(V) concentration was analyzed by spectrophotometric method based on the molybdenum blue. In particular, the analytical solution was prepared by adding: 0.5 g ammonium heptamolybdate (by Sigma Aldrich), 0.04 g potassium antimony tartrate (by Carlo Erba), 4 ml concentrated sulfuric acid (98 wt%, by Sigma Aldrich) and an adequate amount of ascorbic acid (by Carlo Erba), in a total solution volume of 100 ml. Samples were analyzed with a Perkin Elmer UV-Vis spectrophotometer at λ = 880 nm. Slurry samples were collected at fixed time intervals, and filtered (pore size: 0.45 μm) for removing photocatalyst particles. The concentration of As(III) was determined by the difference between total arsenic and As(V) concentration.

3. Results and discussion

3.1. Catalyst characterization

3.1.1. TG–DTG analysis

Table 1 reports the list of catalysts with some characteristics. TG–DTG analysis of MoO_x/TiO_2 catalysts (not reported) showed four main steps of weight loss: (i) the first one associated with hydration water desorption, (ii) the second one related to the removal of hydroxyls surface groups of titania, (iii) the third one attributed to the decomposition of sulphate species giving rise to gaseous SO_3 [26], (iv) the last one attributed to Mo oxide sublimation from TiO_2 surface occurring at temperatures higher than 700 °C [26]. This last step was absent for pristine TiO_2, confirming that it was only due to the presence of Mo-species dispersed on titania surface. Therefore this last step is used to estimate the real content of Mo oxide (Table 1) that is consistent with the nominal MoO_3 content.

3.1.2. Specific surface area measurement

Specific surface areas measured as a function of Mo loading are useful to extract information about monolayer formation [1]. SSA values for MoO_x/TiO_2 catalysts used in the present study are reported in Table 1. It can be seen that surface area of Mo loaded catalysts shows a decreasing trend with increasing Mo content. This decrease is about 7% of the TiO_2 support for the addition of 14.8 wt% molybdenum. However, SSA is constant up to 5.8 wt% Mo loading and beyond this loading it starts to decrease. This trend can be attributed to a progressive aggregation of individual particles during the calcination treatment, decreasing the exposed surface area and the inter-particles porosity [23].

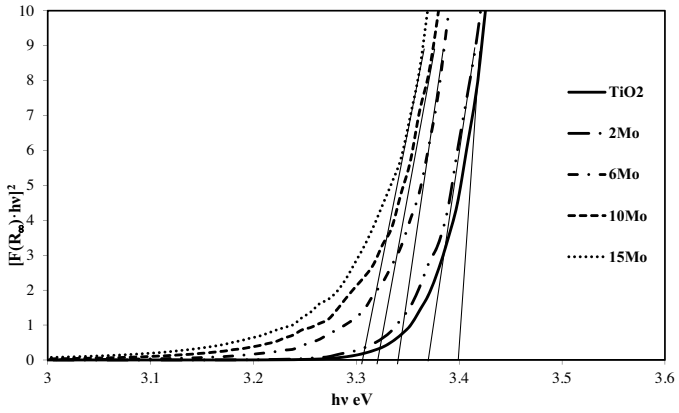

Fig. 1. Band gap calculus from UV–vis DRS spectra.

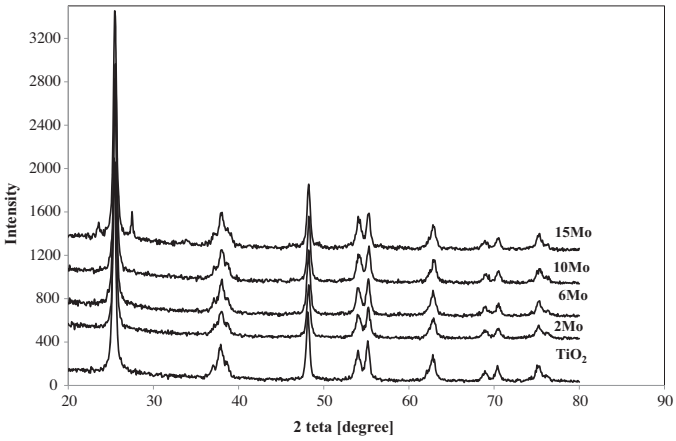

Fig. 2. XRD spectra.

3.1.3. UV–vis DRS results

UV–vis DRS spectra of the photocatalysts evidenced that the surface coverage with MoO_x did not significantly decrease the equivalent band gap energies (E_{bg}) with respect to the relevant support as shown in Fig. 1 and Table 1. In particular E_{bg} was in the range 3.3–3.4 eV. This last result implies that all the prepared catalysts can be only activated by light sources having an emission spectrum in the UV region.

3.1.4. XRD results

The crystalline structure of the catalysts was studied by X-ray diffraction analysis (Fig. 2). Titania support exists within 5% of determination error in anatase phase. No additional peaks due to molybdenum can be observed up to 8.4 wt% Mo-loading. At 14.8 wt%, XRD patterns show two additional diffraction peaks at $2\theta = 23.4$ and 27° due to MoO_3 crystallites [14].

Overall results indicate that the calcination process did not alter the crystallographic phase of the support and that up to 8.4 wt% Mo-loading, molybdenum oxide remained on the surface of titania support as amorphous phases, meaning that it is well dispersed on it.

The average size of TiO_2 crystallites was calculated using the Scherrer equation [15] on diffraction plane (1 0 1). The obtained results are reported in Table 1. Accordingly, the average crystallites size of TiO_2 is 19 nm and 18 nm for all MoO_x/TiO_2 catalysts. The results indicate that the presence of MoO_x species does not restrain the crystallization of the support [27].

3.1.5. Raman analysis

The Raman spectra of the MoO_x/TiO_2 catalysts, in comparison with TiO_2, in the ranges 100–700 and 700–1100 cm^{-1} are shown in Fig. 3a and b.

TiO_2, 2Mo, 6Mo, 10Mo and 15Mo samples display bands at 144, 396, 514 637 cm^{-1} and a weak shoulder at 195 cm^{-1} due to the anatase form of TiO_2 (Fig. 3a) [28]. In the range 700–1100 cm^{-1} TiO_2 support evidenced a band centered at about 800 cm^{-1} assigned to the first overtone of the 396 cm^{-1} anatase mode [29]. In the same range, Raman spectra show main bands at 960 cm^{-1} on 2Mo and at 970 cm^{-1} on 6Mo, characteristic of Mo=O stretching vibrations of hydrated octahedrally anchored species interacting with TiO_2 surface [30]. With the increase of Mo-loading up to 8.4 wt%, the Raman band due to the Mo interaction species narrowed and shifted to about 993 cm^{-1}. The increase of the Raman shift with increasing Mo-loading is due to a progressively higher degree of polymerization of Mo anions [23]. The formation of segregated crystalline MoO_3 is strongly evident from the additional peak at about 820 cm^{-1} observed only for the 15Mo catalyst [23].

Following the method proposed by Quincy et al. [29], the Mo-loading corresponding to the monolayer coverage was evaluated

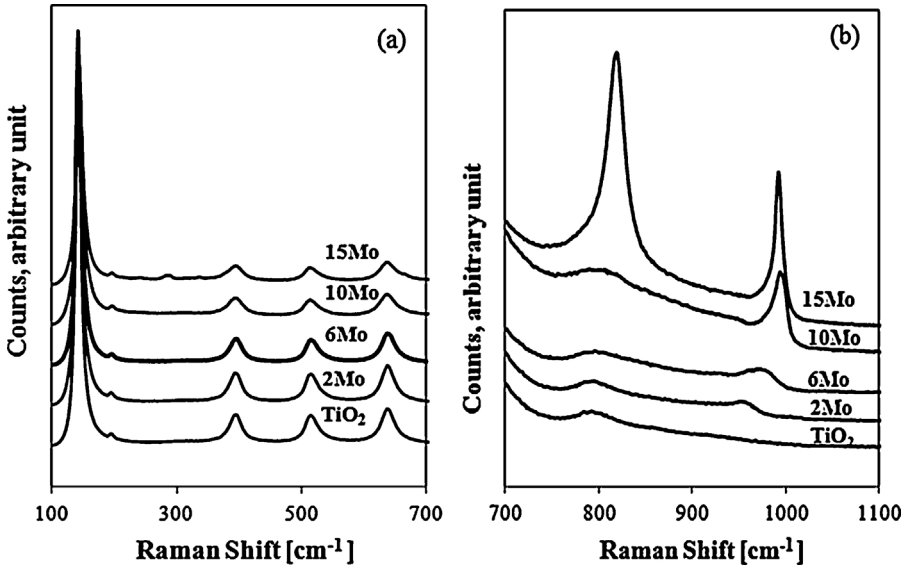

Fig. 3. Raman spectra of the samples in the range 100–700 cm^{-1} (a) and in the range 700–110 cm^{-1} (b).

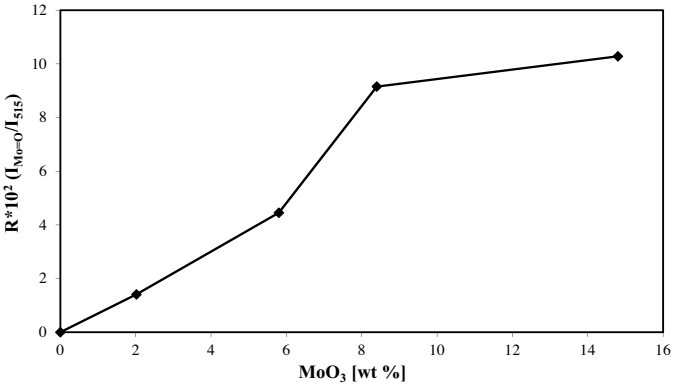

Fig. 4. Raman peak area intensity ratio of the Mo interaction species/PC105 as a function of Mo loading for MoO_x/TiO_2 catalysts.

from the Raman spectra. In Fig. 4, the ratios between the area of the overall Mo-species peaks in the range 920–1005 cm^{-1} and the area of titania peak at 515 cm^{-1} are reported.

An important point to focus in Fig. 4 is that the intensity of Mo interaction species increases with Mo loading up to 8.4 wt% MoO_3 and levels off at higher Mo loadings. This last result indicates that monolayer coverage on the titania PC105 is attained at a MoO_3 loading of about 8.4 wt%, in agreement with a previous study [31] who found, for titania, a molybdenum oxide monolayer coverage of 7.6 μmol/m^2, corresponding to about 7.7 wt% of MoO_3 on PC105 with a surface area of 70 m^2/g, used in the present study.

3.2. Photocatalytic activity tests

3.2.1. Optimization of catalyst dosage for photocatalytic tests

Preliminary tests carried out in dark conditions evidenced only a negligible oxidation activity.

The determination of the optimal catalyst dosage was made under UV irradiation by testing different concentrations of 6Mo photocatalyst, in the range 0.1–0.5 g/L. Moreover aqueous samples containing As(III) were irradiated to determine whether As(III) is oxidized to As(V) also in the absence of catalyst. Fig. 5 shows the conversion of As(III) after 20 min of UV irradiation. The results of the experiments showed that oxidation of As(III) to As(V) also occurred in the absence of photocatalyst, but the reaction was slower than in the presence of the catalytic material. Increasing the amount of catalyst in the solution, a linear increase of photocatalytic efficiency up to a dosage of 0.3 g/L can be observed; beyond the latter value, the conversion remained constant.

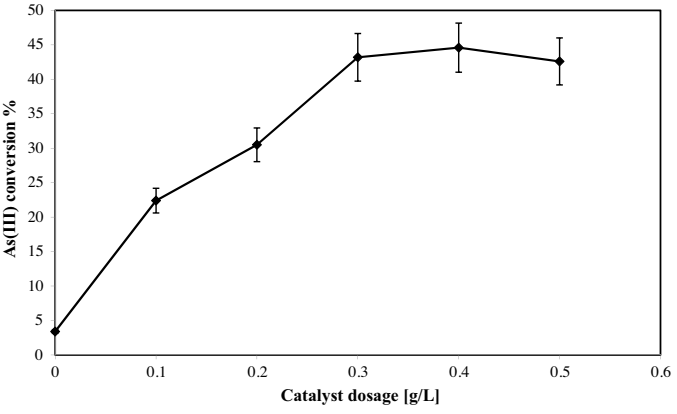

Fig. 5. Evaluation of As(III) conversion after 20 min of irradiation with different 6Mo catalyst dosage and with incident photon flux equal to 7.5 W/m^2.

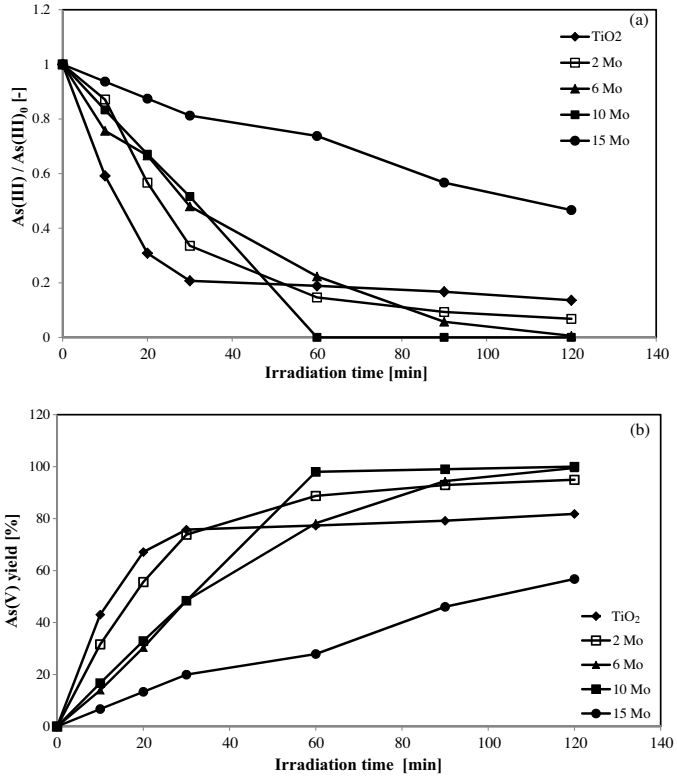

Fig. 6. Behavior of As(III) relative concentration in solution (a) and behavior of As(V) yield (b) as a function of irradiation time for different wt% of MoO_3 and with incident photon flux equal to 7.5 W/m^2.

This phenomenon may be explained considering that with an increase of catalyst loading in the aqueous medium, the light penetration through the solution becomes difficult [6]. Therefore 0.3 g/L of photocatalyst loading was considered as the optimum dose and used to investigate the influence of MoO_3 loading in the absence and in the presence of UV irradiation, and the effect of incident photon flux on photocatalytic performances.

3.2.2. Influence of molybdenum loading

Fig. 6a and b shows the evolution of the As(III) normalized to its initial concentration and As(V) yield as a function of irradiation time. In the case of TiO_2 support, the concentration of As(III) decreased up to 30 min of irradiation, reaching a As(III) conversion and As(V) yield of about 81 and 76%, respectively. After 30 min, As(III)/As(III)$_0$ remained almost constant indicating the TiO_2 is not able to oxidize the totality of As(III) present in solution.

For all Mo-based photocatalysts, the concentration of As(III) decreased and As(V) yield increased up to about 100% during the irradiation time. For irradiation time lower than 30 min, the order of photoactivity was as following: TiO_2 > 2Mo > 6Mo > 10Mo > 15Mo. Therefore, the photocatalytic reaction rate decreased by increasing Mo-loading, in agreement with literature papers concerning photocatalytic reactions in the presence of MoO_x/TiO_2 catalysts in gas–solid system [23]. The behavior is completely different for irradiation times higher than 30 min. In particular the complete oxidation of As(III) to As(V) (100% yield), occurred after 60 min of irradiation for 10Mo catalyst, indicating the existence of an optimal MoO_3 loading.

A very interesting information is obtained by comparing in the same plot the behavior of total arsenic and As(III) normalized concentration with together As(V) yield obtained on TiO_2 and 10Mo photocatalyst (Fig. 7). When UV light was switched on, As(III)

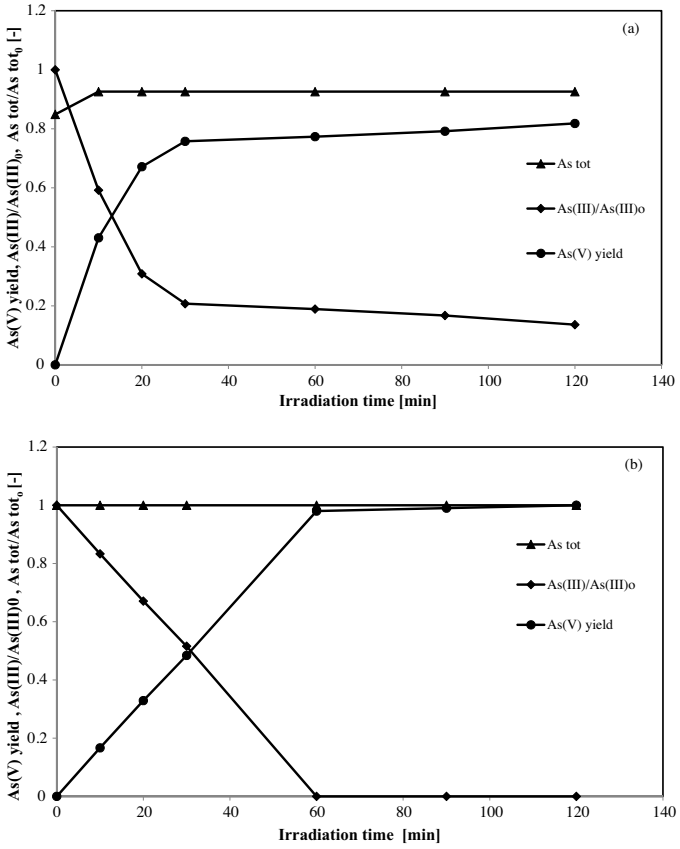

Fig. 7. Behavior of As(III) relative concentration in solution As(V) yield and total arsenic relative concentration as a function of irradiation time for TiO_2 (a) and 10Mo photocatalyst (b) with incident photon flux equal to 7.5 W/m^2.

concentration decreased and As(V) yield increased. For TiO_2, As(III) relative concentration after 60 min was 0.18, corresponding to a conversion of arsenite equal to 81%, higher than As(V) yield, indicating that a fraction of As(V) produced has been adsorbed on TiO_2 surface and, thus, causing the progressive deactivation of the photocatalyst (Fig. 7a). On the contrary, in the presence of 10Mo photocatalyst (Fig. 7b), As(III) concentration decreased and As(V) yield concurrently increased. In parallel, the total arsenic in solution did not change during the irradiation time. This last result clearly shows that As(V) produced by the photo-oxidation of As(III) was completely released into the solution, thus not occupying the active sites of the catalyst, avoiding its deactivation and enhancing its stability.

With the aim to confirm 10Mo stability, photocatalytic performance of the system was investigated for three cycles with the same sample and experimental conditions. From Fig. 8, it can be seen that As(III) conversion of the first and third cycle is about 40% and 39% respectively after 20 min of irradiation. Compared to the first and third cycle, the reaction rate resulted in a quite poor decrease, however comprised in the error bars. This result indicated that photocatalytic rate of 10Mo sample did not decline substantially.

3.2.3. Effect of incident photon flux on photocatalytic performances: hypothesis of reaction mechanism

The influence of incident photon flux on the photocatalytic performances was studied using 10Mo catalyst. Fig. 9 displays the trend As(III) normalized concentration and As(V) yield as a function of irradiation time for different incident photon flux.

The light intensity was varied from 7.5 to 25.5 W/m^2 (by varying the distance between the light source and water surface). At fixed

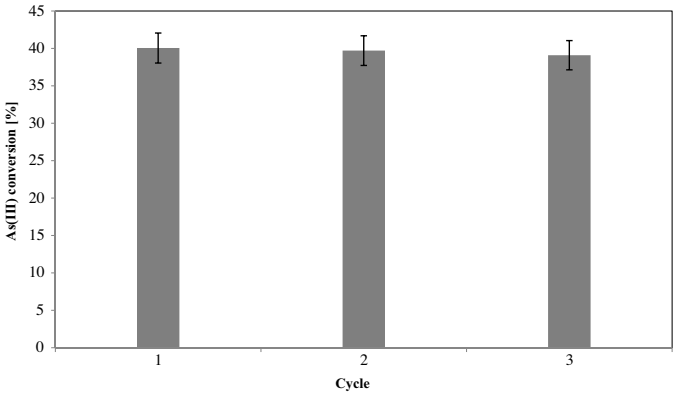

Fig. 8. Evaluation of As(III) conversion after 20 min of irradiation on 10Mo catalyst for different cycles and with incident photon flux equal to 7.5 W/m^2.

irradiation time, the As(III) oxidation rate and As(V) yield decreased with the increase of incident photon flux. This behavior is in contrast with the typical trend observed in the photocatalytic oxidation of As(III) with the increase of light intensity and in the presence of TiO_2 suspension [32]. The explanation of the previous result was found out firstly by observing a color change (from white-yellow to blue-gray) of the catalyst at the end of the photocatalytic test with an incident photon flux of 11.5 and 25.5 W/m^2. This color change was attributed to the photoreduction of molybdenum, in particular to the formation of molybdate blue, a well known phenomenum related to reduced isopolymolybdate complexes, containing both Mo(V) and Mo(VI) [33].

Thus, according to the results in Fig. 9, it is clear that the effectiveness of the photoreaction decreased when molybdate was photoreduced, suggesting that MoO_x species act as a redox catalyst in the photocatalytic oxidation of As(III), as previously found in the photo-oxidation of cyclohexane to benzene on MoO_x/TiO_2

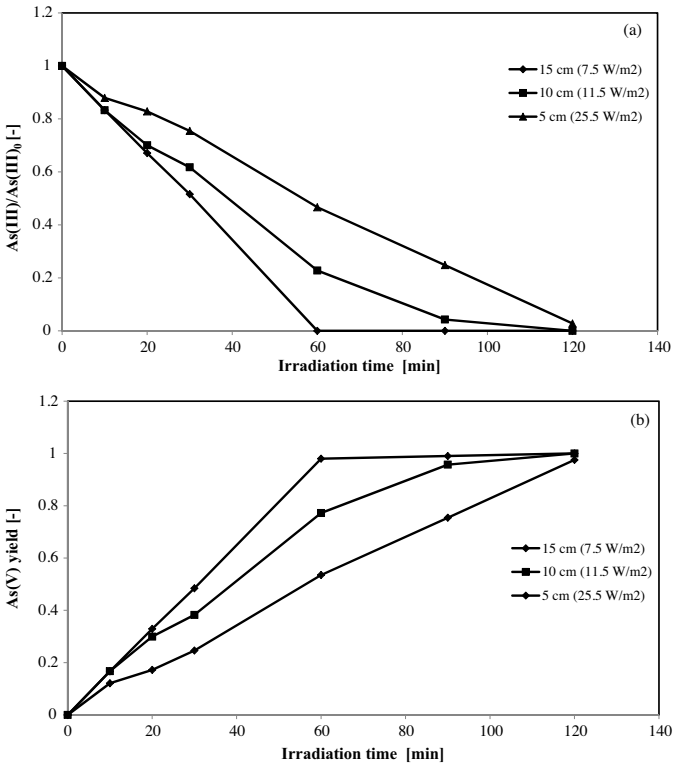

Fig. 9. Trend of As(III) relative concentration (a) and As(V) yield (b) as a function of irradiation time for different incident photon flux for 10Mo.

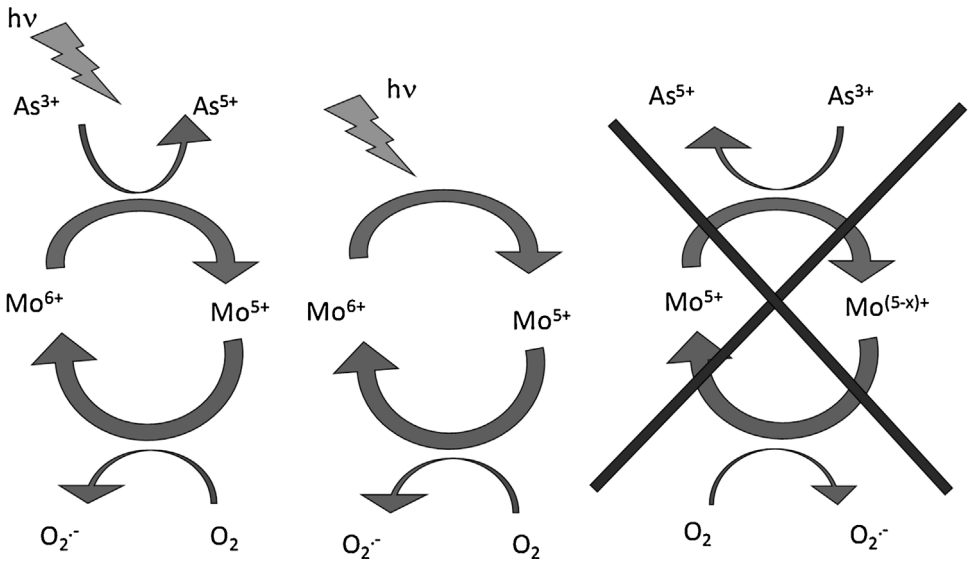

Fig. 10. Schematic picture of the reaction mechanism in the presence of MoO_x and UV light.

and ethanol to acetaldehyde on VO_x/TiO_2 [23,34]. More specifically, with the increase of the UV light flux, the molybdate, Mo^{6+} is reduced to Mo^{5+}, and the reoxidation occurs slower than the reduction due to the concurrent oxidation of As. This reaction depends on the level of oxygen present, so, it could be expected, that the reduction will be limited in the presence of a higher amount of oxygen. Accordingly, polymolybate with Mo in the state 6+ is the active site and the reoxidation of formed Mo(V) is the rate limiting step.

The possible mechanism of reaction involving both molybdate and titania can be explained according to the following Eqs. (1)–(8). The oxidation of As(III) into As(V) on bare titania may occur through the mechanism proposed in literature (Eqs. (1)–(6)) [17], in which the holes generated by UV irradiation oxidize As(III) into As(IV) (Eq. (4)). As(IV) is subsequently oxidized to As(V) by superoxides (Eq. (5)) and by hydroxyl radicals (Eq. (6)).

$$TiO_2 + h\nu \rightarrow e^- + h^+ \quad (1)$$

$$e^- + O_2 \rightarrow O_2^{\bullet -} \quad (2)$$

$$h^+ + OH^- \rightarrow OH^{\bullet} \quad (3)$$

$$As(III) + h^+ \rightarrow As(IV) \quad (4)$$

$$As(IV) + O_2^{\bullet -} \rightarrow As(V) \quad (5)$$

$$As(IV) + OH^{\bullet} \rightarrow As(V) \quad (6)$$

Simultaneously, the photoexcited polymolybdate is reduced by the electron migrated into the conduction band (Eq. (7)). The reduced molybdate rapidly reacts with O_2 present in the reaction medium bringing molybdate in the initial oxidation state and producing superoxides (Eq. (8)), which can react with As(IV) according to Eq. (6).

$$MoO_x + e^- \rightarrow MoO_x^- \quad (7)$$

$$MoO_x^- + O_2 \rightarrow MoO_x + O_2^{\bullet -} \quad (8)$$

The reaction mechanism in the presence of MoO_x and UV light is schematized in Fig. 10.

If the catalyst surface is poor oxygenated, and in the presence of very high photon flux, the kinetic of Eq. (8) is much lower than that of Eq. (7), leaving a lesser number of superoxides able to oxidize As(IV) and, consequently, leading to a decrease of the photocatalytic performances.

These observations can explain the results reported in Fig. 9.

4. Conclusions

Photocatalytic oxidation of As(III) into As(V) in mild conditions has been studied in the presence of supported Mo catalysts. The formation of polymolybdate species spread on the anatase surface increases with increasing molybdenum loading up to the monolayer formation. In this case, the complete oxidation of As(III) to As(V) occurred after 60 min of irradiation, whereas titania alone was not able to oxidize the totality of As(III) present in solution.

The increase of photo-efficiency in the presence of MoO_x/TiO_2 samples could be ascribed to the enhanced superoxide generation induced by surface molybdate that works as electron shuttle between the conduction band of TiO_2 and O_2 present in the reaction medium. After monolayer formation, segregation of MoO_3 crystallites was observed with a significant loss in photocatalytic activity. Moreover, the overall As(V) produced on MoO_x/TiO_2 catalysts is completely released into solution, then not going to occupy the active sites allowing to formulate a photocatalyst with high stability over the time. These results make the photocatalytic process with MoO_x/TiO_2 a really attractive option for the oxidation of As(III) to As(V) in drinking water due to its high stability over time and consequently lower operating costs compared to traditional catalysts.

Acknowledgements

The authors wish to thank University of Salerno for funding the project “(Ex 60%, anno 2011). Processi chimici catalitici per la produzione di energia sostenibile e l’ambiente”. Luigi Rizzo wish to thank University of Salerno for funding the project “Rimozione dell’arsenico dalle acque ad uso potabile mediante un processo combinato e simultaneo di ossidazione fotocatalitica e adsorbimento” (Ex 60%, anno 2013).

References

[1] G. Liu, X. Zhang, J.W. Talley, C.R. Neal, H. Wang, Water Res. 42 (2008) 2309–2319.
[2] A. Nikolaou, L. Rizzo, H. Selcuk, Control of Disinfection By-Products in Drinking Water Systems, Nova Science Publishers, Inc., Hauppauge, NY, 2007.
[3] L. Rizzo, D. Sannino, V. Vaiano, O. Sacco, A. Scarpa, D. Pietrogiacomi, Appl. Catal. B: Environ. 144 (2014) 369–378.
[4] V. Vaiano, O. Sacco, M. Stoller, A. Chianese, P. Ciambelli, D. Sannino, Int. J. Chem. React. Eng. 12 (2014) 1–13.

[5] D. Sannino, V. Vaiano, P. Ciambelli, Curr. Org. Chem. 17 (2013) 2420–2426.
[6] D. Sannino, V. Vaiano, O. Sacco, P. Ciambelli, J. Environ. Chem. Eng. 1 (2013) 56–60.
[7] J.J. Murcia, M.C. Hidalgo, J.A. Navío, V. Vaiano, D. Sannino, P. Ciambelli, Catal. Today 209 (2013) 164–169.
[8] Y. Ruzmanova, M. Stoller, A. Chianese, Chem. Eng. Trans. 32 (2013) 2269–2274.
[9] Y. Ruzmanova, M. Ustundas, M. Stoller, A. Chianese, Chem. Eng. Trans. 32 (2013) 2233–2238.
[10] M. Stoller, K. Movassaghi, A. Chianese, Chem. Eng. Trans. 24 (2011) 229–234.
[11] F. Parrino, G. Camera-Roda, V. Loddo, G. Palmisano, V. Augugliaro, Water Res. 50 (2014) 189–199.
[12] V. Augugliaro, M. Bellardita, V. Loddo, G. Palmisano, L. Palmisano, S. Yurdakal, J. Photochem. Photobiol. C: Photochem. Rev. 13 (2012) 224–245.
[13] M. Hajaghazadeh, V. Vaiano, D. Sannino, H. Kakooei, R. Sotudeh-Gharebagh, P. Ciambelli, Catal. Today 230 (2014) 79–84.
[14] D. Sannino, V. Vaiano, P. Ciambelli, P. Eloy, E.M. Gaigneaux, Appl. Catal. A: Gen. 394 (2011) 71–78.
[15] V. Palma, D. Sannino, V. Vaiano, P. Ciambelli, Ind. Eng. Chem. Res. 49 (2010) 10279–10286.
[16] M. Bissen, M.M. Vieillard-Baron, A.J. Schindelin, F.H. Frimmel, Chemosphere 44 (2001) 751–757.
[17] H. Lee, W. Choi, Environ. Sci. Technol. 36 (2002) 3872–3878.
[18] T.V. Nguyen, S. Vigneswaran, H.H. Ngo, J. Kandasamy, H.C. Choi, Sep. Purif. Technol. 61 (2008) 44–50.
[19] S. Bang, M. Patel, L. Lippincott, X. Meng, Chemosphere 60 (2005) 389–397.
[20] G.-h. Moon, D.-h. Kim, H.-i. Kim, A.D. Bokare, W. Choi, Environ. Sci. Technol. Lett. 1 (2014) 185–190.
[21] D. Sannino, V. Vaiano, P. Ciambelli, G. Carotenuto, M. Di Serio, E. Santacesaria, Catal. Today 209 (2013) 159–163.
[22] D. Sannino, V. Vaiano, P. Ciambelli, Catal. Today 205 (2013) 159–167.
[23] D. Sannino, V. Vaiano, P. Ciambelli, J.J. Murcia, M.C. Hidalgo, J.A. Navío, J. Adv. Oxid. Technol. 16 (2013) 71–82.
[24] M. Antoniadou, V. Vaiano, D. Sannino, P. Lianos, Chem. Eng. J. 224 (2013) 144–148.
[25] D. Sannino, V. Vaiano, P. Ciambelli, Res. Chem. Intermed. 39 (2013) 4145–4157.
[26] P. Ciambelli, D. Sannino, V. Palma, V. Vaiano, Int. J. Photoenergy 2008 (2008).
[27] E. Rahmani, A. Ahmadpour, M. Zebarjad, Chem. Eng. J. 174 (2011) 709–713.
[28] L.J. Alemany, L. Lietti, N. Ferlazzo, P. Forzatti, G. Busca, E. Giamello, F. Bregani, J. Catal. 155 (1995) 117–130.
[29] R.B. Quincy, M. Houalla, D.M. Hercules, J. Catal. 106 (1987) 85–92.
[30] M. Cheng, F. Kumata, T. Saito, T. Komatsu, T. Yashima, Appl. Catal. A: Gen. 183 (1999) 199–208.
[31] I.E. Wachs, Catal. Today 27 (1996) 437–455.
[32] P.K. Dutta, S.O. Pehkonen, V.K. Sharma, A.K. Ray, Environ. Sci. Technol. 39 (2005) 1827–1834.
[33] T. He, J. Yao, J. Photochem. Photobiol. C: Photochem. Rev. 4 (2003) 125–143.
[34] P. Ciambelli, D. Sannino, V. Palma, V. Vaiano, R.S. Mazzei, Photochem. Photobiol. Sci. 8 (2009) 699–704.